[1]Shuzhen Wang*
[1]Yuren Chen
[1]Yinglun Chen

Collaborative planning of data center and energy storage based on i-C&CG solving algorithm

JES Journal of Electrical Systems

Abstract: - With the rapid development of new power systems and advanced technologies such as artificial intelligence, the penetration rate of renewable energy is increasing, and the electricity consumption required for computing power calculation is surging. On the one hand, the uncertainty of wind power output has in-creasingly serious impact on the operation safety of power system. On the other hand, internet data center (IDC) needs to consume a lot of power to maintain the computing power system. Therefore, a two-stage robust collaborative programming model of IDC and BESS with life constraints is proposed herein. Plan storage capacity and data center server configuration with the goal of minimizing system operation and planning costs. An inexact column-and-constraint generation (i-C&CG) algorithm is proposed herein to solve the problem, and the IEEE-30 nodes system is simulated. The planning considering the life constraints of BESS are more reasonable, and i-C&CG algorithm can reduce the difficulty of solving two-stage robust planning problem of power system.

Keywords: Wind power output uncertainty; Internet data center; Life constraints of BESS; i-C&CG algorithm.

I. Introduction

power to support the safe and stable operation of the computing system in all aspects. By 2021, the total energy consumption of the IDC in China has reached 2.6% of the total annual electricity [3]. On the other hand, its computing load has a large spatiotemporal schedulability and can be used as a flexible resource to improve system flexibility [4,5]. In recent years, some scholars have proposed that IDC can collaborate with power grid flexibility resources such as battery energy storages (BESS) to optimize power system flexibility and reduce system operation or planning costs [6-9].

At present, in the relevant research on collaborative planning of IDC and energy storage, BESS has attracted much attention from scholars due to its advantages such as fast response, high efficiency and flexible location selection [10-14]. In order to realize the collaborative planning of IDC and BESS, scholars explore the methods of collaborative planning of the IDC and BESS with the goal of improving system economy, flexibility and data center service quality. [12] proposes the shared operation mode of BESS of IDC alliance, and studied the optimal capacity allocation and BESS planning of IDC under the collaborative optimization of IDC and BESS. [13] considers the collaborative planning of IDC and BESS, and builds a multi-objective model. Results show that the use of the spatio-temporal load transfer flexibility of IDC to coordinate the planning of the location and scale of BESS can significantly improve the service quality, economy and reliability of the system. The above researches mainly considers the planning costs of BESS, but does not introduce the server capacity configuration of IDC into the planning objectives, failing to make full use of their collaborative planning advantages.

In order to further explore the collaborative planning method of IDC and BESS, some scholars conducted researches on scenarios such as AC and DC power supply and fault operation conditions from the perspective of power grid operation reliability, and verified the advantages of collaborative planning of IDC and BESS in improving power system reliability [15-17]. [18-19] incorporated the cost of IDC and BESS into the planning objectives, and through collaborative planning, reduced the total planning cost of IDC and BESS, reduced the number of idle servers, and reduced the configuration requirements of BESS. Although the above researches provide sufficient theoretical basis for solving the problem of collaborative planning between IDC and BESS, the impact of BESS life loss cost is not considered. In addition, the above researches only consider the

[1] *Corresponding author: Shuzhen Wang, *102110341@hbut.edu.cn*
Author Affiliation: Hubei Engineering Research Center for Safety Monitoring of New Energy and Power Grid Equipment, Hubei University of Technology, Wuhan, China

transferable and reducible capabilities of IDC, and did not distinguish the demand response characteristics of the time transferable computing load and space transferable computing load of IDC [20], which misestimated the response capability of IDC and required further improvement of the model.

Moreover, considering the uncertainty of renewable energy, scenario-based stochastic programming [21-22] and robust programming [23-24] are widely adopted. However, stochastic programming needs to generate multiple scenarios to represent uncertainty, and it requires accurate probability distribution of random variables, which increases the difficulty of calculation. However, robust programming only considers the worst scenario, and although the calculation is simple, the result is conservative. In order to avoid overly conservative results, some scholars adopt a two-stage robust programming method for research, that is, the main problem solves the planning objective. The sub-problem considers the worst variation of the uncertain parameters to verify the rationality of the second-stage robust optimization results. Repeated iterations can ensure that the optimization results fall into local optimal solutions [25-27]. In [28], for the mixed integer programming in the subproblem, KKT conditions are added to the main problem, and then the duality is performed to obtain the subproblem, so as to avoid the MLIP problem of the subproblem. [29] solves the two-stage robust optimization problem with integer subproblems, and realized the transformation of integer variables by constructing the inner and outer layer subproblems and using KKT conditions for duality. When solving the two-stage robust planning problem of microgrid, most of the above literatures only consider the possible adjustments in the sub-problems, but lack of consideration for the optimization in the process of solving the main problem.

In summary, a load-storage collaborative planning scheme considering BESS life constraints and IDC demand response is proposed herein. Firstly, transitive characteristics present in time and space of IDC and the influence of BESS charging and discharging strategy on its lifetime are researched, and the demand response constraints of IDC and BESS are constructed. Then, the location and capacity planning model of IDC and BESS is established, and the embedded operation model introduces the energy storage life constraint into the model. In the planning stage, the optimal capacity of IDC and the optimal location and capacity of BESS are studied with the goal of economic optimization. In the running stage, a two-stage robust optimization model is constructed considering the system operation under the worst case of IDC adjustable capacity and renewable energy output. Finally, an faster inexact column-and-constraint generation (i-C&CG) algorithm is proposed to improve the computing speed of the model and solve some difficult problems in the two-stage robust planning process of power system.

II. Methodology

2.1. The space-time transfer feature of IDC data load

IDC can use the data network to realize the rapid transfer of data load, which affects the power demand of IDC and realizes the transfer of power load. Generally, data loads undertaken by IDC can be divided into delay-tolerant loads, quality-tolerant loads and rigid loads according to the user's delay time tolerance [30]. The response characteristics of the above three types of loads will be further described in detail in the following sections.

2.1.1. Response Characteristics of TSDL

Time-Shiftable Data Load (TSDL) means that the data load only needs to complete the processing within a certain time limit, and the user has a high tolerance for the processing time. For IDC, most common delay-tolerant loads are batch loads.

In the power system scheduling cycle, the delay-tolerant load can delay the processing time of the data load within a reasonable range, and the process can only be delayed backward, not processed in advance. That is, the delay-tolerant load at time t can be postponed to [t+1,T] for processing, which can be expressed as load proportion of delay-tolerant load, data transfer constraints before and after response, and total transferable constraints of delay-tolerant load respectively.

$$L_{i,t}^{Bat0} = \beta_1 L_{i,t}^{0} \tag{1}$$

$$L_{i,t}^{Bat} = L_{i,t}^{Bat0} + \sum L_{i,t't}^{Bat} - \sum L_{i,tt'}^{Bat} \tag{2}$$

$$\sum L_{i,tt'}^{Bat} \le \beta_1 L_{i,t}^{0} \tag{3}$$

here, $L0\ i,t$ is the total data load received by IDC; β_1 is the proportion of delay-tolerant load in total data task; $LBat0\ i,t$ is the initial quantity of TSDL; $LBat\ i,t't$ is the data task capacity transferred from time t to time t'; $LBat\ i,t$ is the delay-tolerant data amount at the end of scheduling.

2.1.2. Response Characteristics of STDL

Space transferable data load (STDL) means that when a processing request occurs, the data load needs to be processed in a fixed time, but the quality of the server is low, and the transfer work can be realized between different IDCs. Generally, the data load is not strict to the computing power and quality requirements.

In the power system scheduling cycle, the quality tolerant load can rely on the data network to realize the spatial transfer of the data load. Quality tolerance load response and processing should be started at the same time, and load transfer tasks can only be achieved through data transmission. Equations (4) to (6) respectively represent the proportion of the capacity load of the quality tolerance type, the data transfer constraint before and after the response, and the total quantity constraint that the quality tolerance type load can be transferred.

$$L_{i,t}^{ST0} = \beta_2 L_{i,t}^{0} \tag{4}$$

$$L_{i,t}^{ST} = L_{i,t}^{ST0} + \Sigma L_{ji,t}^{ST} - \Sigma L_{ij,t}^{ST} \tag{5}$$

$$\Sigma L_{i,t}^{ST} \le \beta_2 L_{i,t}^{0} \tag{6}$$

β_2 is the proportion of the quality tolerant load in the total data task; $LST0\ i,t$ is the initial quantity of TSDL; $LST\ ji,t$ is the data task capacity transferred from IDC_i to IDC_j; $LST\ i,t$ is the quality tolerance data amount of IDC_i at the end of scheduling.

2.1.3. Response Characteristics of Rigid Loads

Some data loads are time-sensitive and require high data processing quality, so they cannot be transferred in time and space. This type of data load is called a rigid load and must be completed locally as soon as the task is received. Therefore, rigid loads are not flexible and cannot participate in demand response during the power system scheduling cycle. Generally, the rigid load is mostly the urgent and important data load. The operating characteristics of rigid loads are as follows:

$$L^{Base} = (1-\beta_1-\beta_2)L_{i,t}^{0} \tag{7}$$

Where, L^{Base} is the rigid load of IDC_i at time t, that is, the difference between the initial load and the initial load of other loads.

Therefore, the IDC load after participating in the demand response can be described as:

$$L_{i,t} = L_{i,t}^{Bat} + L_{i,t}^{ST} + L_{i,,t}^{Base} \tag{8}$$

Where, $L_{i,t}$ is the total data load after IDC_i participates in demand response at time t.

2.2. BESS Response Characteristics Considering Lifetime Constraints

The life loss of BESS during the operation is different under the influence of different charging and discharging strategies. The number of BESS cycles varies with different discharge depths [31-32]. Therefore, the rain-flow counting method is used here to determine the cyclic discharge depth of BESS [33] and calculate the corresponding cycle life. The influence of charge and discharge decision on cycle life of BESS is described by introducing cyclic action variable.

2.2.1. Life Constraints of BESS

BESS will be affected by side reactions caused by its own charge and discharge during operation, resulting in fluctuations or even imbalances in the battery capacity balance. The above process is affected by the depth of discharge and can be accumulated through circulation. The functional relationship between cycle life and cycle discharge depth is power-rate variation.

$$N_{life} = N_0 \left(DoD_{cyc} \right)^{-k_p} \tag{9}$$

Where, N_{life} is the number of cycles when the battery reaches the end of life; N_0 is the number of cycles when the battery reaches the end of life when charging and discharging at 100% discharge depth; DOD_{cyc} indicates the actual cyclic discharge depth

$$y_{Ech} + y_{Edch} \le 1 \tag{10}$$

of the battery; k_p is curve fitting parameter; N_0 and k_p are the inherent constants of the battery.

But in actual work, the cycle discharge depth is not a fixed value, and only the maximum discharge depth replaces the cycle discharge depth, which will cause a large error. In order to study the influence of different

charge and discharge cycles, each cycle discharge can be converted to the equivalent total cycle number n_{eq} at 100% discharge depth. According to Equation 9, the equivalent number of full cycles is:

$$n_{eq} = DoD_{cyc}{}^{k_p} \tag{11}$$

The number of equivalent cycles per day can be obtained by superimposing the number of equivalent cycles.

$$N_{eq} = \sum_t n_{eq} \tag{12}$$

The cycle life of BESS can be obtained from the daily equivalent cycle number N_{eq} of BESS.

$$T_{cyc} = \frac{N_0}{365 N_{eq}} \tag{13}$$

Where, T_{cyc} is the cycle life of BESS, and the unit is year.

2.2.2. Actual Cyclic Discharge Depth Model

The actual cyclic discharge depth is the discharge depth of the BESS at the last moment when the BESS is transferred from the discharge process to the charging process. Among them, the discharge depth is the ratio of the output power of BESS to the total capacity, that is, it is related to the state of charge.

$$DOD = (1 - SOCE) \tag{14}$$

Where, *DOD* is the actual discharge depth, *SOCE* is the state of charge of BESS.

After introducing the charge and discharge cycle identifier *SE*, the actual cycle discharge depth can be indicated

$$DOD_{cyc}^{t} = DOD_t \cdot SE_t \tag{15}$$

DODt cyc is the discharge depth of BESS at time *t*. When *SE* is 1, the number of discharge times is recorded, indicating that BESS transitions from discharge to charge and the discharge process of BESS ends. Therefore, the cyclic charge and discharge mark can be described as follows:

$$SE^{t} = \max\left\{ y_{E,ch}^{p,t} - y_{E,ch}^{p,t-1}, 0 \right\} \tag{16}$$

Where, the value of *yp,t E,ch* is 1, indicating that BESS is in the charging process at time *t*.

In order to describe the specific charge and discharge behavior of BESS, it is necessary to describe the relationship between the charging state, discharge state and rest state of BESS and the charging process and discharge process. During operation, in order to ensure the energy continuity of BESS, it can only be in the charging or discharging process. During the charging process, the BESS may be in a continuous charging state, or it may end the charging state and enter a static state. During the discharge process, BESS may be in a continuous discharge state, or it may end the discharge state and enter a static state. It can be described as:

$$y_{Ech}^{P} + y_{Edch}^{P} = 1 \tag{17}$$

$$y_{E,dch}^{P,t} \geq y_{E,dch}^{P,t-1} - y_{E,dch}^{t} - y_{E,ch}^{t} \tag{18}$$

$$y_{E,ch}^{P,t} \geq y_{E,ch}^{P,t-1} - y_{E,dch}^{t} - y_{E,ch}^{t} \tag{19}$$

$$y_{E,dch}^{P,t} \geq y_{E,dch}^{t} \tag{20}$$

$$y_{E,ch}^{P,t} \geq y_{E,ch}^{t} \tag{21}$$

When, *yt E,ch* is 1, it means that BESS*t* is in the charging state at all times, and when *yt E,dch* is 1, it means that BESS is in the discharging state at all times. When both are 0, the state is at rest.

Therefore, based on the charging state of BESS and the cycle frequency of charge and discharge, the cyclic discharge depth of BESS is correlated with the depth of single discharge and the charge and discharge action of BESS, and the cyclic discharge depth model of BESS is constructed.

III. Two-Stage Robust Planning Model of Collaboration Between IDC and BESS

3.1. Objective Function

Bulleted lists look like this:Aiming at the lowest equivalent daily planning and total operating cost in the planning period, a collaborative planning configuration model of BESS-IDC is established. The planning cost includes the IDC server construction cost C_{IDC} and the BESS construction cost C_{ESS}. The total operating cost mainly includes the start-up cost of thermal generator unit C_{G1}, the operating cost of thermal generator unit C_{G2}, and the IDC response cost $C_{IDC\text{-}grid}$.

$$\min \quad C_{IDC} + C_{G1} + C_{G2} + \max \min C_{ESS} + C_{IDC-grid} + C_{G3} \tag{22}$$

$$C_{IDCN} = \frac{r(1+r)^{Y_{IDC}}}{r(1+r)^{Y_{IDC}} - 1} M_i^{ser} \theta^{I-ser} \tag{23}$$

$$C_{IDC} = \frac{C_{IDCN}}{365} \tag{24}$$

$$C_{ESSN} = c_E EE \cdot e_E \frac{\mathrm{r}(1+r)^{T_{cyc}}}{\mathrm{r}(1+r)^{T_{cyc}} - 1} \tag{25}$$

$$C_{ESS} = \frac{C_{ESSN}}{365} \tag{26}$$

$$C_{G1} = u_g SU \tag{27}$$

$$C_{G2} = a_g y_g \tag{28}$$

$$C_{G3} = b_g P_g \tag{29}$$

$$C_{IDC-grid} = c \sum_i \sum_{t'=t+1}^{T} L_{i,t}^{Bat}(t'-t) \tag{30}$$

Where, r is the discount rate; Y_{IDC} indicates the server life of an IDC; $\Theta^{I\text{-}ser}$ indicates the cost of a single server at an IDC; SU is the start-up cost of thermal generator set; a_g is the online cost of thermal generator set; b_g is the cost generated by the operation of thermal generating units.; c is the response incentive cost of IDC.

3.2. Constraint

3.2.1. Constraints on Power Balance

$$\Sigma P_{g,i}^t + EE * e_E \Sigma (P_{dch} - P_{ch}) = P_{load}^{n,t} + \Sigma P_{ij}^t + PIDC \tag{31}$$

$$P_{ijlow} \le P_{ij}^t \le P_{ijup} \tag{32}$$

Where, P_{dch} and P_{ch} are the average charging and discharging power of BESS; *PIDC* is the total power consumption of IDC; *Pn,t load* is the load of node *n*; *Pt ij* is the power flow of line *ij*; P_{ijup} and P_{ijlow} are the upper and lower limits of power flow for each line; *EE* is the BESS capacity reference value, and e_E is the total configured BESS capacity.

3.2.2. Constraints of Thermal Generating Units

Reserve constraint of thermal power generation

$$\Sigma (P_{ga}^t - Q17 * P_g^t) >= R * \Sigma P_{load}^t \tag{33}$$

Power-on identification constraint

$$-y_{g,i}^{t-1} + y_{g,i}^t - u_{g,i}^t <= 0 \tag{34}$$

$$u_{g,i}^t \le y_{g,i}^t \tag{35}$$

$$u_{g,i}^t \le 1 - y_{g,i}^t \tag{36}$$

Constraints on upper and lower limits of output

$$y_{g,i}^t P_{g,i}^{low} \le P_{g,i}^t \le P_{ga,i}^t \le y_{g,i}^t P_{g,i}^{up} \tag{37}$$

Climbing constraint

$$P_{ga,i}^t - P_{g,i}^{t-1} \le RU \tag{38}$$

$$-P_{ga,i}^t + P_{g,i}^{t-1} \le RD \tag{39}$$

Start and stop time constraints

$$y_{g,i}^k \ge y_{g,i}^t - y_{g,i}^{t-1} \quad 1 \le k - (t-1) \le \min \mathrm{up} \tag{40}$$

$$1 - y_{g,i}^k \ge y_{g,i}^{t-1} - y_{g,i}^t \quad 1 \le k - (t-1) \le \min \mathrm{down} \tag{41}$$

Where, *Pt ga* is the standby output of thermal power generation at time *t*; *Pt g* is the actual output of thermal power generation at time *t*; *R* is the standby capacity; *yt g,i* is the online identifier of thermal generator set *i*. When the value is 1, it indicates that the thermal generator set is in working state. *yt g,i* is the startup identifier of the thermal generator set, and the value is 1 if and only when the thermal power generation is switched from shutdown to operation. In addition, *RU*, *RD*, minup, mindown, *Plow g,i* and *Pup g,i* are respectively the climbing and sliding rates, the minimum on-off time and the upper and lower limits of output of the thermal generating units.

3.2.3 Constraints of IDC Server Running and Planning

As a high energy user, IDC's energy consumption is mainly composed of servers, refrigeration equipment and power distribution equipment. Among them, servers and refrigeration equipment account for the highest proportion of energy consumption. Generally, power utilization efficiency (PUE) is used to describe the power consumption relationship of servers within an IDC. PUE is defined as the ratio of total power consumption to server power consumption.

$$PIDC = \alpha P^{ser} \tag{42}$$

Where, P^{ser} is the power consumption caused by the operation of a server inside a IDC;α is the power utilization rate of IDC.

The power consumption of IDC servers can be calculated based on the number of servers that are powered on and the data load that servers can carry. Assuming that each server works only in the standby state and rated power consumption state, the server power consumption is calculated as follows:

$$P^{ser} = M^{ser-on} P^{ser-idle} + (P^{ser-peak} - P^{ser-idle}) \frac{L_{i,t}}{\tau_i} \tag{43}$$

Where, $M^{ser\text{-}on}$ indicates the number of startup servers; $P^{ser\text{-}idle}$ indicates the static power consumption of servers in the IDC; $P^{ser\text{-}peak}$ indicates the rated power consumption of the server; $L_{i,t}$ is the data load carried by IDCi at time t; τ_i is the service efficiency of the server.

The upper limit for the number of servers that can be started must meet the configuration requirements of the IDC, and the data loads that can be carried by different IDCs must be within their respective processing capabilities.

$$M^{ser-on} \le M^{ser} \tag{44}$$

$$0 \le L_{i,t} \le M^{ser} U^{\max} \tau_i \tag{45}$$

Where, M^{ser} is the total number of servers in the IDC; U^{max} indicates the maximum processing efficiency of a single server.

Assume that servers in the same IDC are of the same type and meet the $M/M/1$ queue theory.

$$T_{i,t}^{Q} = \frac{1}{\tau_i - \frac{L_{i,t}}{M_{i,t}^{Ser-on}}} \tag{46}$$

$$T_{i,t}^{H} = \frac{1}{\tau_i} \tag{47}$$

$$T^{Q} + T^{H} \le T^{Del} \tag{48}$$

Where, T^Q is the queuing time; T^H is the processing time; T^{Del} is the average time required for data processing. The minimum number of servers on power is restricted as follows:

$$M^{ser-on} \ge \frac{L_{i,t}}{\tau_i (1 - \frac{1}{\tau_i T_{Del} - 1})} \tag{49}$$

3.2.4 Operation and Planning Constraints of BESS

In order to study the location and capacity planning of BESS, node investment identifier ZE and capacity allocation quantity e_E of BESS are introduced. Therefore, the charging constraint of BESS can be rewritten as:

$$DOD^{t} = ZE(1 - SOCE^{t}) \tag{50}$$

And add operational investment constraints:

$$ZE \ge y_{Ech} \tag{51}$$

$$ZE \ge y_{Ech} \tag{52}$$

Charge status constraints:

$$SOCE^{t} = SOCE^{t-1} + (P_{ch}^{t} \eta_{ch} - \frac{P_{dch}^{t}}{\eta_{dch}}) \tag{53}$$

$$ZE * SOCE_{low} \le SOCE \le ZE * SOCE_{up} \tag{54}$$

Charge and discharge constraint of BESS:

$$0 \le P_{ch} \le y_{Ech} P_{ch}^{up} \tag{55}$$

$$0 \le P_{dch} \le y_{Edch} P_{dch}^{up} \tag{56}$$

The equilibrium constraint of beginning and end of BESS:

$$SOCE^{ter} = ZE \cdot SOCE^{ini} \tag{57}$$

Where, η_{ch} and η_{dch} are the charge and discharge efficiency of BESS; $SOCE_{up}$ and $SOCE_{low}$ are the upper and lower limits of BESS capacity; *Pup ch* and *Pup dch* are the upper limit of charging and discharging power of BESS; $SOCE^{ter}$ indicates the initial charging state; $SOCE^{ini}$ is the last charged state.

3.3. Solving The Imprecise Column and Constraint Generation Method for Two-Stage Robust Optimization Problem

3.3.1. Two-stage robust optimization model

The two-stage robust collaborative planning abstract model of IDC and BESS can be expressed as:

$$\min \quad c_1 x \quad + \max_{d} \min_{y} \quad c_2 y \tag{58}$$

$$\begin{aligned} & Ax \geq b \\ s.t \quad & Ey \geq h \\ & By + Dx \geq d \end{aligned} \tag{59}$$

Where, A, B, D and E represent the coefficient matrix of each constraint respectively; b, h and d are the parameter vectors of the corresponding constraints. The constraints of the first stage include the operating state of BESS (equation (15) - (21)), the operating constraints of thermal power generation (equation (31) - (33) (37) (38)), and the operating state of BESS (equation (48) (49)). The constraints of the second stage include the load classification of the IDC (equation (1) - (8)), BESS life (equation (9) - (12)), backup and ramp of thermal power generation (equation (30) (35) (36)), power of the IDC server (equation (39) (40)), and queue constraints (equation (46)). The variable constraints of the second stage including the first stage are as follows: cyclic discharge depth (equation (47) (14), power balance constraint (equation (28) (29)), output upper and lower limit constraint (equation (34)), server construction constraint (equation (41) (42)) and BESS operation constraint (equation (50) - (54)).

Deterministic models are often more risky, and the influence of uncertainty should be taken into account in the model. The uncertainty can be described as:

$$d_{low}^{t} \leq d^{t} \leq d_{up}^{t} \tag{60}$$

$$\sum_{t=1}^{T} \left| \frac{d^{t} - d_{low}^{t}}{d_{low}^{t}} \right| = \varphi \tag{61}$$

Where, d^t is the net load at time t; *dup t* and *dlow t* are the upper and lower limits of the fluctuation range of d^t; T is the scheduling time period; φ is the uncertainty.

3.3.2. An i-C&CG algorithm

For the above two-stage robust optimization model, due to the difficulty in solving the main problem, the i-C&CG algorithm is adopted herein [34]. i-C&CG algorithm is similar to C&CG) algorithm in that the alternate solution of the original problem consists of a main problem and a subproblem. The difference between the two lies in that i-C&CG algorithm adds relative uncertainty gap $\varepsilon_{\mathrm{MP}}$ to solve complex problems in the process of solving the main problem, so as to improve the calculation speed. A new backtracking process is introduced in the iterative process to test the feasibility and applicability of the imprecise solution.

By decomposing equation (61-62), the main problem form is obtained as:

$$MP: \min \quad c_1 x_j + \mu_j \tag{62}$$

$$\begin{aligned} & Ax_j \geq b \\ s.t \quad & \mu_j \geq c_2 y_j \\ & Ey_j \geq h \\ & By_j + Dx_j \geq d_j \\ & c_1 x_j + y_j \geq LB \end{aligned} \tag{63}$$

Where, j is the initial value of the number of iterations of the loop is 1, and l is the initial value of the current number of iterations is 0; μ_j is the optimal value obtained by solving the objective function of the subproblem, which will pass the worst scenario d_j to the main problem participation constraint. *LB* is used to improve the lower bound value of the main problem, which is initially set to 0.

When the main problem is solved with the relative optimal gap $\varepsilon_{\mathrm{MP}}$, the solver can calculate the optimal solution obtained by integer continuity, denoted as the upper bound U_j of the main problem; And the solution when the current solver obtains the integer, denoted as the lower bound L_j of the main problem, and L_j should be greater than or equal to LB. If satisfied:

$$L_j > LB \tag{64}$$

To update the current iteration number, let $l=j$.

After completing the comparison of formula (65), LB is updated so that $LB=U_j$. The optimal decision value x_j is recorded. After the main problem is solved successfully, the sub-problem is solved based on x_j. However, because the subproblem is maxmin problem, it cannot be solved directly. Therefore, KKT conditions are introduced here to achieve the solution.

$$SP: \min \quad c_2 y \tag{65}$$

$$\begin{aligned} & Ey \geq h \\ s.t \quad & Ey - h \leq Mv_1 \\ & \pi_1 \leq M(1-v_1) \\ & \pi_1 \leq c_2 \\ & By + Dx_s \geq d \\ & By + Dx_s - d \leq Mv_2 \\ & \pi_2 \leq M(1-v_2) \\ & \pi_2 \leq c_2 \end{aligned} \tag{66}$$

In the formula, π_1 and π_2 are dual variables, and v_1 and v_2 are linearized variables introduced by the large M method after using KKT conditions. x_s indicates the result of a phase. M is a very large number. Record the optimal objective function value D_j, the worst scenario d_j, and update the upper bound of the original problem.

$$UB = \min\left\{UB, c_1 x_j + D_j\right\} \tag{67}$$

When the actual relative gap is close enough, i.e

$$(UB - L_l)/UB < \varepsilon \tag{68}$$

Where, ε is the specified tolerance, when equation (69) is satisfied, the iteration ends and the original problem is identified as the optimal solution. If ε is not satisfied, then the imprecise relative difference must be compared, i.e

$$(UB - U_j)/UB < \varepsilon_1 \tag{69}$$

Where, ε_1 is the imprecise tolerance, and in order to ensure the reliability of the imprecise relative gap, the value of ε_1 should be satisfied

$$0 < \varepsilon_1 < \varepsilon/(1+\varepsilon) \tag{70}$$

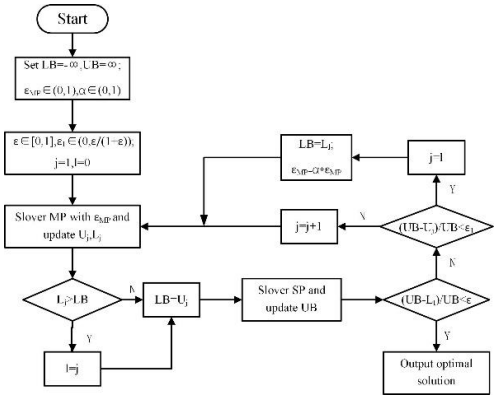

Figure 1. Initial input data of the system

When the solution results meet the equation (71), $j=l$, $LB=L_l$, reduce the relative optimal gap $\varepsilon_{MP}=\alpha \cdot \varepsilon_{MP}$, and then return to solve the main problem for iteration.

If the imprecise relative difference is not satisfied, the worst scenario is updated and the main problem is returned for iteration. (See **Figure 1**)

IV. Results and discussion

4.1 Parameter Settings

MATLAB and Yalmip environments are used here for solving. The CPU of the computer is i5-10300H CPU, and the solver uses gurobi10.0.2 for calculation.

To verify the effectiveness of the proposed method, a modified IEEE-30 node power system is simulated. As shown in Figure 2, the system consists of 21 load nodes, 6 thermal generating units, and 3 data centers.

Among them, the thermal generator set is linked to nodes 1, 2, 5, 8, 11, 13, and the IDC is connected to nodes 3, 14, and 25.

Each unit of the system is shown in Table 1, including the main parameters of different subsystems such as thermal generator set, IDC and BESS [32].

Table 1. Parameters of each system unit

Thermal power units								
Unit number	Pup g/MW	Plow g/MW	RU/ RD	mindown	minup	a_g/$	b_g/$	SU/$
1	157	50	37.5	4	4	244.2	20.26	3200
2	100	25	30	4	4	244.2	20.26	3200
3	60	15	15	3	3	176.8	24.68	3000
4	80	20	20	3	3	176.8	24.68	3000
5	40	10	15	2	2	120	40	7000
6	40	10	15	2	2	120	40	7000
BESS								
P_{chup}/P_{dchup}	5MW	Discount rate r	5%					
EE	10MW	$SOCE_{min}$	0.25					
η_{ch}/η_{dch}	0.95/1	$SOCE_{max}$	1					
C_E	18250$	eE_{max}	3					
N_0	1591	T_{flo}	10					
k_p	2.09							
IDC								
β_1/β_2	0.1/0.1	T_{del}	0.1s					
Y_{IDC}	10year	τ	500 $s^{(-1)}$					
α	1.5	c	0.01$/Gbit					
P_{peak}	15kW	$\theta^{l\text{-}ser}$	8030$					
P_{idle}	7.5kW	T_{IDC}	10year					

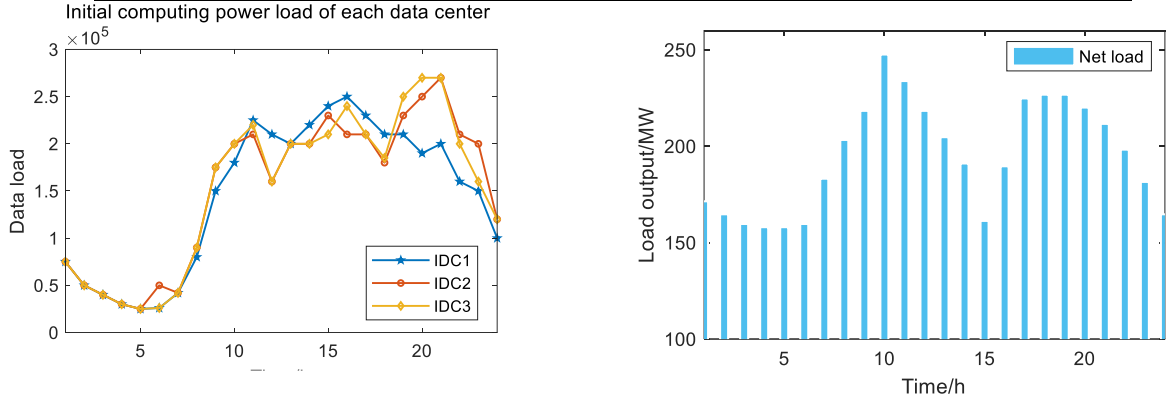

Figure 2. Initial input data of the system

4.2 Simulation Analysis

4.2.1 Consider the Advantages of Load-Storage Collaborative Planning Strategy

In order to verify the effectiveness of the collaborative planning model established herein, we explore the improvement of the flexibility and economy of the power system by collaborative planning. Set the following scheme for simulation comparison:

Case 1: Do not consider the transfer capability of IDC load, and do not consider the BESS configuration;

Case 2: Only consider the planning of BESS, without considering the transfer capability of IDC load;

Case 3: Only consider the planning after IDC participates in the demand response, and do not configure the BESS system.

Case 4: The collaborative planning model of IDC and BESS proposed herein.

The result of IDC and BESS are shown in Table 2, including the daily equivalent total cost. C_{G1} is the online fixed cost of thermal generating units; C_{G3} is the amount operating cost of thermal generating units; C_{BESSN} is the annual equivalent construction cost of energy storage; $C_{IDC\text{-}gird}$ is the incentive cost of data centers; C_{IDCN} is the annual equivalent construction cost of data centers.

Table 2. Comparison of cost results under different planning cases

Cost/$	**case 1**	**case 2**	**case 3**	**case 4**
Total cost	176725	166134	169008	161591
Fixed cost of unit	20468	19324	21000	18970
Variable cost of the unit	151196	134600	145943	132812
Annual investment cost of energy storage		606995		567210
Incentive costs for data centers			1845.8	1830
Annual investment cost for data center	1846900	1846900	1558915	1557820

The above comparison results show that the comprehensive cost of case 4 is the lowest, indicating that the collaborative planning of IDC and BESS has good economy. Among them, the proportion of the cost of thermal generating units in the total equivalent daily cost is the most advanced. Compared with Case 1, the configuration of flexible resources can effectively reduce the demand for thermal power generation, but IDC is limited by the high proportion of its own rigid load, and the adjustable capacity of IDC is not as good as the adjustment capacity of BESS. By comparing the construction investment cost of IDC in four different cases, it can be concluded that the construction of IDC is mainly affected by its own computing power load, and the participation of IDC in demand response can greatly reduce the demand for IDC.

The annual equivalent construction cost of BESS in Case 4 decreased by $39,785 compared to Case 3, while the annual equivalent construction cost of IDC decreased by $1,105 compared to Case 3. Comparative analysis shows that the collaborative planning of IDC and BESS can not only reduce the energy consumption requirements of IDC, but also reduce the configuration requirements of BESS and server capacity. In addition, in the comparison between Case 4 and Case 3. It is because the configuration of BESS can promote the spatial transferable load of servers in IDC to participate in demand response flexibly, so as to improve the load demand response capability of IDC internal servers and reduce the corresponding incentive cost.

In order to further reveal the impact of collaborative planning between IDC and BESS on the configuration requirements of BESS, the location capacity and cycle life of BESS in Case 4 and Case 2 are counted, as shown in Table 3.

Table 3. BESS configuration in different cases

case 2							
Life/year	6	4	6	10	7	7	7
Site	4	6	14	19	24	25	27
Capacity/MW	30	30	20	30	30	30	20
case 4							
Life/year	8	9	5	9	6	7	10
Site	1	8	9	24	25	26	28
Capacity/MW	30	30	30	30	20	30	30

As can be seen from Table 3, in Case 2, because IDC does not participate in demand response, BESS needs to sacrifice its cycle life to meet the flexibility requirements of the system. Case 2 had a mean life span of 5.86, and Case 4 had a mean BESS life span of 7.71. In Case 2, the life cost will limit the capacity allocation of BESS. Although the total investment construction cost is not higher than that in Case 4, the total cost is higher than that in Case 4. In addition, compared with the site selection of the two Cases, the site selection of Case 2 is closer to the IDC, which is convenient for load side peak regulation, while the BESS of Case 4 is mainly near the thermal power node, which is more conducive to smooth thermal power output and improve the system's ability to consume new energy.

In order to analyze the influence of the collaborative planning of IDC and BESS on the operation decision of IDC, the output of each IDC under the planning scheme of Case 3 and Case 2 and the total load of IDC are counted, as shown in Figure 3.

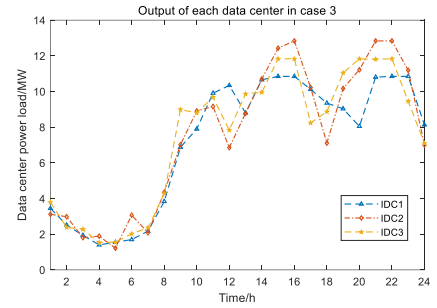

a Load of IDC in Case 3

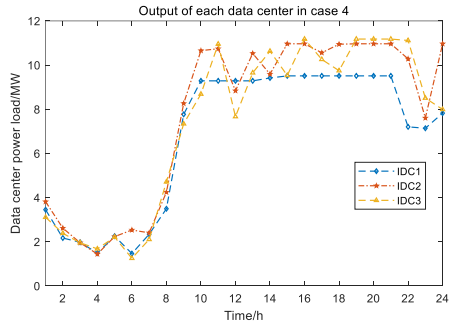

b Load of IDC in Case 4

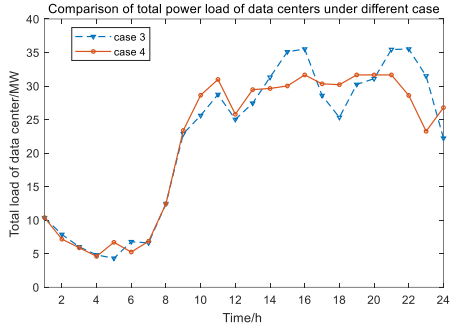

c Total load of IDC

Figure 3. Output analysis of IDC

By comparison, it can be found that in Case 4, the load difference between peak and valley of IDC is small, which is 25MW. IDC's peak was slightly lower, at 30MW. In Case 2, the total load peak of the IDC is high due to the large fluctuation between IDC2 and IDC3 between 15:00 and 20:00. But in Case 4, after BESS is configured, the load of the IDC can be adjusted by a mass tolerance load, which has a smoother output between 10:00 and 20:00 with smaller peaks. As a result, the total number of servers required for Case 4 is reduced. The collaborative planning of IDC and BESS can give full play to the flexibility of both and reduce the configuration requirements of both.

4.2.2 Influence of BESS Life Constraints on Planning Results

In order to study the impact of BESS life constraints on the planning results and further verify the effectiveness of the collaborative planning model proposed herein, the IDC and BESS collaborative planning model, which does not consider the life of BESS, are

respectively compared with the collaborative planning modeling method proposed herein. The cost comparison results of the two methods are shown in Table 4.

Table 4. Costs with CMP and EQU

Cost	control group（CMP）	experimental group（EQU）
Total cost/$	161932	162592
Fixed cost of unit/$	17732	18970
Variable cost of the unit/$	131478	132812
The total number of e_E/uint	18	22

It is assumed that the service life of all BESS is 10 years in the CMP model, and other constraints are consistent with EQU. According to Table 4, since CMP does not consider the life loss cost of BESS, it will overestimate the adjustable capacity of BESS, and the total capacity of BESS is less than the EQU model, which may lead to the problem of insufficient capacity of BESS. In the CMP model, the flexibility of the system is too optimistic. Compared with the EQU model, the online cost of thermal power is reduced by $3005. At the same time, the total cost is reduced by $1250, and the thermal power operating cost is reduced by $1334. If the life of BESS is not considered, the regulation capacity of BESS will be optimistically estimated, and then the thermal power output decision-making will be affected.

In order to study the influence of BEESS life constraints on BESS regulation capacity, the total BESS output is calculated, as shown in Figure 4.

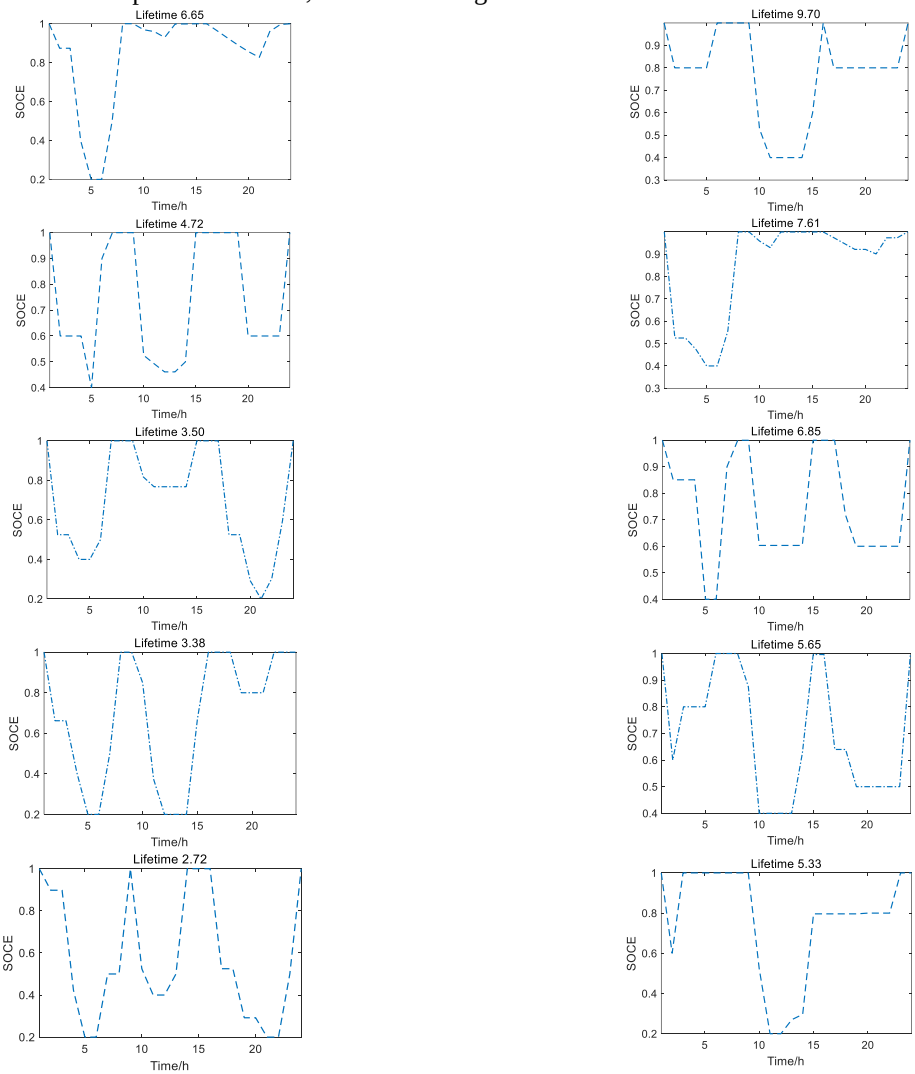

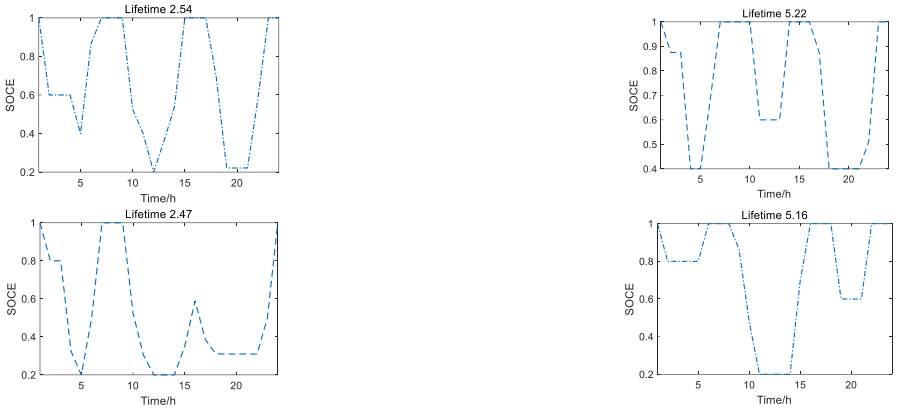

(a)CMP (b)EQU

Figure 4. Total output of energy storage

Compared with the total output of BESS under the two models in Figure 4, when the model does not consider the life loss cost, the depth of BESS discharge increases, the discharge frequency increases, and the life of BESS decreases significantly. The maximum cycle life of BESS in EQU model is 9.7 years. The maximum BESS cycle life of CMP model is 6.65 years, and the BESS life of CMP model is obviously worse than that of EQU model. Therefore, considering the BESS life loss cost can avoid overestimating the adjustable capacity of BESS and improve the reliability of the model.

4.2.3 Advantages of i-C&CG Algorithm in Solving Two-Stage Robustness Problem of Power System

In order to improve the computational speed of two-stage robust main problem of power system, the column and constraint generation algorithm is improved by introducing imprecise relative gap and backtracking check history. The iteration speed of i-C&CG algorithm and C&CG algorithm under the time limit of single computation and the final convergence difference under the same initial inaccuracy are compared herein. The advantages of i-C&CG algorithm for two-stage robust programming are explored.

The C&CG algorithm with the initial gap of 0.16 and 0.18, the initial gap of 0.18, the precision adjustment coefficient of 0.9, the convergence gap of 0.04, the relative gap of 0.05, the single calculation time of 4000s, and the total number of iterations limited to 8 are solved for the collaborative planning problem of IDC and BESS in Case 4 of the above calculation examples.

The i-C&CG algorithm can greatly reduce the difficulty of the initial solution of the main problem. In the initial stage of solving, the i-C&CG algorithm has low accuracy, so the solving speed is similar to the C&CG algorithm with low precision. With the increase of the number of iterations, i-C&CG algorithm can constantly check the rationality of the solution accuracy setting through the backtracking process, and constantly improve the solution accuracy. It can be analyzed from Figure 5 that after the end of the third iteration, the calculation results of the i-C&CG algorithm are basically stable, and the solution time begins to drop significantly. This is because the i-C&CG algorithm determines that the i-C&CG algorithm result is close to the optimal solution through verification, so the solution accuracy is automatically updated, and the calculation result is more accurate, and the time required for solving the near-optimal solution is greatly reduced. Compared with the iterative results with the initial accuracy of 0.16, it is not difficult to find that the gap between the calculation results of the i-C&CG algorithm and the results of the C&CG algorithm with high precision is gradually shortened, which once again verifies the effectiveness of the i-C&CG algorithm.

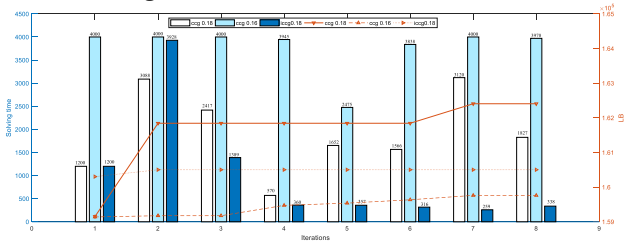

Figure 5. Comparison of algorithm solving speed

V. Conclusion

In order to improve the flexibility and reliability of IDC-BESS collaborative planning, a two-stage robust microgrid planning model for IDC-BESS collaborative planning considering the life constraints of BESS is proposed. Compared with existing studies, BESS life constraints are incorporated into the model in this paper to avoid overly optimistic results and improve the reliability of planning results. The advantages of IDC and BESS collaborative planning are studied from the perspective of the flexibility and economy of the grid side, and the advantages of two different flexibility resources are analyzed. Finally, the i-C&CG algorithm is proposed to solve the two-stage robust planning problem of microgrid. According to the simulation analysis of the example, the main conclusions are as follows:

(1) Compared with the independent planning of IDC or BESS, the collaborative planning of both can effectively improve the operational flexibility of microgrids. In the face of large fluctuations in renewable energy, IDC and BESS collaborative planning is less costly than planning alone. IDC reduces the configuration requirements of BESS through load transfer, and improves the overall system economy.

(2) After considering the life constraint of BESS, in order to avoid overcharge and overdischarge behavior, thermal generating units need to provide more energy, and the configuration requirement of BESS increases. The results show that the BESS programming model with life constraints can ensure the reliability and economic optimization of the planning results.

(3) After i-C&CG algorithm is adopted, the difficulty of solving the main problem of the two-stage robust planning model of microgrid is reduced, and the results of i-C&CG algorithm are more accurate than those of C&CG algorithm under the same time limit. With the same accuracy, i-C&CG algorithm can automatically adjust the relative gap, so the total calculation time is shorter. Comparing the two algorithms to solve the two-stage robust planning problems of different microgrids, the analysis results show that the i-C&CG algorithm is more advantageous when it is difficult to solve the main problem of two-stage robust planning of microgrids..

REFERENCES

[1] Q.H. Huang, S.Q. Shao, H.N. Zhang and C.H. Tian, “Development and composition of a data center heat recovery system and evaluation of annual operation performance,” Energy, vol. 189, no. 15, pp. :116200, 2019.

[2] X.F. Huang, J.W Yan, X. Zhou, Y.X. Wu and S.C. Hu, “Cooling Technologies for Internet Data Center in China: Principle, Energy Efficiency, and Applications,” Energies, vol. 16, no. 20, pp. :7158, 2023.

[3] W.L. Ni, X.R. Hu, H.Y. Du, Y.L. Kang, Y. Ju and Q.W. Wang, “CO_2 emission-mitigation pathways for China's data centers,” Resour. Conserv. Recy., vol. 202, no. 1, pp. :107383, 2024.

[4] J. Jian, J.L. Zhao, H.R. Ji, L.Q. Bai, J. Xu, P. Li, J.Z. Wu and C.S.Wang, “Supply restoration of data centers in flexible distribution networks with spatial-temporal regulation,” IEEE Trans. Smart Grid, vol. 15, no. 1, pp.:340–354, 2024.

[5] J.X. Wan, J. Zhou and X. Gui, “Sustainability analysis of green data centers with CCHP and waste heat reuse systems,” IEEE Trans. Sustainable Comput., vol. 6, no.1, pp:155–167, 2021.

[6] B. Robert, “Flexibility-Based Energy and Demand Management in Data Centers: A Case Study for Cloud Computing,” Energies, vol. 12, no. 17, pp:3301, 2019.

[7] H.J. Gao, X.D. Lyu, S.J. He, L.F. Wang, C. Wang and J.Y.Liu, “Integrated planning of cyber-physical active distribution system considering multidimensional uncertainties,” IEEE Trans. Smart Grid, vol. 13, no.4, pp:3145–3159, 2022.

[8] X. Zhao, Z.Q. Bai, W.L. Xue, N. Xu, C.H. Li and H.R. Zhao, “Research on bi-level cooperative robust planning of distributed renewable energy in distribution networks considering demand response and uncertainty,” Energy Rep., vol. 7, no. 7, pp:1025–1037, 2021.

[9] X.Y. Yang, X.Y. Song, M.K. Liao, X.Y. Liu and Q. Guo, “Hybrid Energy Storage Configuration of Wind Power Microgrid: A Strategy based on the EMD technique and Two-stage Robust Method,” Sci. Rep., vol. 14, no. 1, pp:2733, 2024.

[10] X.X. Long, Y.Z. Li, Y. Li, L.J. Ge, B.G. Hoay, C.Y. Chung and Z.G. Zeng, “Collaborative Response of Data Center Coupled With Hydrogen Storage System for Renewable Energy Absorption,” IEEE Trans. Sustain. Energ., vol. 15, no. 2, pp:986-1000, 2024.

[11] R. Giulianno, L. Alexandre, K. Evangelos, F. Gianluca, M. Marco, D. Maurizio and M. Marcelo, “Modeling a Large-Scale Battery Energy Storage System for Power Grid Application Analysis,”

Energies, vol. 12, no. 17, pp. :3312, 2019.
[12] Y.L. Xie, Y. Cui, D.J. Wu, Y.K. Zeng and L.L.Sun, "Economic analysis of hydrogen-powered data center," Int. J. Hydrogen Energ., vol. 46, no. 2 pp:27841-27850, 2021.
[13] K.L. Zhou, Z. Fei and X.Lu, "Optimal energy management of internet data center with distributed energy resources," IEEE Trans. Cloud Comput., vol. 11, no. 3, pp:2285-2295, 2023.
[14] S.T. Wu, Q. Wang and B. Chen, "Collaborative planning of cyber physical distribution system considering the flexibility of data centers," Energy Rep., vol. 9, no. 1 pp:656-664, 2023.
[15] X.H. Liu, G.S.Hou and L.Yang, "Combination optimization of green energy supply in data center based on simulated annealing particle swarm optimization algorithm," Front. Earth Sci., vol. 11, no. 1, pp. :1134523, 2023.
[16] Z.Y. Wang, Y. Wang, H.R. Ji, M.H. Hany, J.L. Zhao, L. Yu, J.F. He, H. Yu and P.Li, "Distributionally robust planning for data center park considering operational economy and reliability," Energy, vol. 290, no. 1, pp. :130185, 2024.
[17] W.B. Qi, J. Li, Y.Q. Liu and C. Liu, "Planning of distributed internet data center microgrids," IEEE Trans. Smart Grid, vol. 10, no. 1, pp. :762-771, 2019.
[18] A.L. Mohammad, A. Shahin, A. Mohsen, Z. Yang, T.B. Payam, A. Ahmad, R. Amin, B. Michael and L. Sebastian, "Energy cost optimization of globally distributed internet data centers by copula-based multidimensional correlation modeling," Energy Rep., vol. 9, no. 1, pp:631-644, 2023.
[19] C.S. Guo, F.L. Luo, Z.X. Cai, Z.Y. Dong and R. Zhang, "Integrated planning of internet data centers and battery energy storage systems in smart grids," Appl. Energy, vol. 281, no. 1, pp. :116093, 2021.
[20] Y.Y. Zhang, B. Zeng, Y.Y. Zhou, H. Xu and W.X. Liu, "Research on Interactive Integration Planning of Data Centers and Distribution Network Driven by Carbon Emission Reduction," Proceedings of the CSEE, vol. 38, no. 23 pp:6433-6450, 2023.
[21] K. Soongelo, "Ensuring renewable energy utilization with quality of service guarantee for energy-efficient data center operations," Appl. Energy, vol. 276, no. 15, pp. :115424, 2020.
[22] Z.H. Ding, Y.J. Cao, L.Y. Xie, Y. Lu and P. Wang, "Integrated stochastic energy management for data center microgrid considering waste heat recovery," IEEE Trans. Ind. Appl., vol. 55, no. 3, pp. :2198–2207, 2019.
[23] D. Erick, Y.Y. Ye, "Distributionally robust optimization under moment uncertainty with application to data-driven problems," Operations Res., vol. 58, no. 3, pp. 595–612, 2010.
[24] J. Muhammad, B.Q. Muhammad, U.S. Muhammad, M.A. Sahibzada, H. Arshad, K. Bilal, X. Wang and U.K. Samee, "A robust optimization technique for energy cost minimization of cloud data centers," IEEE Trans. Cloud Comput., vol. 9, no. 2, pp. :447–460, 2021.
[25] Y. An, B. Zeng, Y. Zhang and L. Zhao, "Reliable pmedian facility location problem: two-stage robust models and algorithms," Transp. Res., Part B, vol. 64, no. 1, pp. :54–72, 2014.
[26] B. Du, H. Zhou and L.Leus, "A two-stage robust model for a reliable pcenter facility location problem," Appl. Math. Model, vol. 77, no. 1, pp. :99–114, 2020.
[27] X. Zhang, X. Liu, "A two-stage robust model for express service network design with surging demand," Eur. J. Oper. Res., vol. 299, no. 1, pp. :154–167, 2022.
[28] Z. Marco, J.C. Antonio, "A robust optimization approach to energy and reserve dispatch in electricity markets," Eur. J. Oper. Res., vol. 247, no. 2, pp. :659–671, 2015.
[29] Q. Zhou, J. Zhang, P. Gao, R. Zhang, L. Liu, S. Wang, L. Chen, W. Wang and S. Yang, "Two-stage robust optimization for prosumers considering uncertainties from sustainable energy of wind power generation and load demand based on nested C&CG algorithm," Sustainability, vol. 15, no. 12, pp. :9769, 2023.
[30] C.S. Guo, F.J. Luo, Z.X. Cai, and Z.Y.Dong, "Integrated energy systems of data centers and smart grids: State-of-the-art and future opportunities," Appl. Energy, vol. 301, no. 1, pp. :117474, 2021.
[31] Y.Y. Shi, B.L. Xu, D. Wang, and B.S. Zhang, "Using battery storage for peak shaving and frequency regulation: Joint optimization for superlinear gains," IEEE Trans Power Syst., vol. 33, no. 3, pp. :2882-2894, 2018.
[32] Y. Ge, C. Shang, "Energy storage planning constrained by its life," Proceedings of the CSEE, vol. 40, no. 19, pp. :6150-6160, 2020.
[33] D. Inderjeet, B. Venkatesh, "Short-term scheduling of thermal generators and battery storage with depth of discharge-based cost model," IEEE Trans. Power Syst., vol. 30, no. 4, pp. :2110-2118, 2015.
[34] Y.T. Man, S.S. Karmel and E.C. Frank, "An inexact column-and-constraint generation method to solve two-stage robust optimization problems," Oper. Res. Lett., vol. 51, no. 1, pp. :92-98, 2023.